Femtosecond Solvation Dynamics of the Hydrated Electron

Carlos Silva, Peter K. Walhout, Kazushige Yokoyama, and Paul F. Barbara*

Department of Chemistry, University of Minnesota, Minneapolis, Minnesota 55455

(Received 8 May 1997; revised manuscript received 24 September 1997)

Femtosecond pump-probe spectroscopy of the equilibrated hydrated electron has been recorded with 35 fs resolution, revealing unprecedented transient features on the 30–80 fs time scales that have been assigned to inertial solvation dynamics of the hydrated electron. These data allow for a rigorous experimental evaluation of the recently published nonadiabatic quantum molecular dynamics simulations of the adiabatic and nonadiabatic dynamics of the hydrated electron. [S0031-9007(98)05313-7]

PACS numbers: 78.47.+p, 31.70.Dk, 33.50.Hv, 82.20.Mj

The hydrated electron is a unique prototype for quantum structure and dynamics in condensed phases. The electronic structure, the static and dynamic spectroscopy, the photoejection and trapping chemistry, and many more aspects of the hydrated electron are receiving intense theoretical and experimental interest [1–19]. Equilibrated hydrated electrons reside in an approximately spherical solvent cavity. They are characterized by a broad, featureless absorption spectrum centered at 720 nm which covers most of the visible and tails into the near-infrared. The majority of the oscillator strength of this absorption derives from optical transitions from the s-like ground state to a set of three nearly degenerate p-like excited states [7,20,21].

Much of the recent research on the hydrated electron has been focused on a new approach to investigate the radiationless relaxation and solvation of excess electrons, namely, the measurement of dynamical spectral changes following photoexcitation from the equilibrated s state to the p-like excited states [22]. This experiment consists of a UV "synthesis" laser pulse producing excess electrons by photodetachment from a solute negative ion. After a fixed delay, during which excess electrons are allowed to thermalize, a femtosecond *pump pulse* promotes them from the ground s state to the p states. The subsequent spectral changes are recorded with a tunable, variably delayed femtosecond laser *probe pulse.* Hydrated electron data derived from this photoexcitation scheme have demonstrated that both transient solvation and the $p \rightarrow s$ radiationless relaxation contribute to the observed spectral dynamics [23]. Results from published photoexcitation experiments were limited, however, to a time resolution of ~300 fs, which *is too slow to resolve much of the theoretically predicted relaxation dynamics.*

This paper represents the first pump-probe measurements on the hydrated electron with ~35 fs resolution. The measurements were made with a homebuilt multipass Ti:sapphire laser system producing 25 fs, 300 μJ laser pulses centered at 800 nm at a repetition rate of 1 kHz [24]. The fourth harmonic of a Q-switched Nd:YLF laser (263.5 nm) photoejected excess electrons from potassium ferrocyanide. All transients were corrected for small artifactual signals centered at zero delay caused by pump-induced phase modulation of the probe [22], which were typically $<1\%$ of the total signal, and as large as 5% in a few cases.

Pump-probe absorption transients of the solvated electron in H_2O and D_2O over a broad range of probe wavelengths, with 35 fs time resolution, are displayed in Fig. 1. The data exhibit dramatic, *previously unobserved dynamics* at all wavelengths probed; see Table I. (At times longer than 300 fs the data are consistent with previous measurements.) The physical significance of the newly observed dynamics can be understood in terms of the prevailing model for the pump-probe spectroscopy of the hydrated electron which is based on molecular dynamics simulations; see Schwartz and Rossky [3–6] and related work from Bratos, Borgis, and co-workers [8,9]. In this model the key dynamical processes and time scales are schematically represented as follows:

$$\text{“}s_{\text{eq}}\text{”} \xrightarrow{h\nu} \text{“}p_{\text{fc}}\text{”} \xrightarrow[\substack{\text{adiabatic}\\ \text{solvation}}]{25-300\ \text{fs}} \text{“}p_{\text{eq}}\text{”} \xrightarrow[\substack{\text{nonadiabatic}\\ \text{transition}}]{\sim 1\ \text{ps}} \text{“}s_{\text{hot}}\text{”} \xrightarrow{\ll 100\ \text{fs}} \text{“}s_{\text{eq}}\text{”}, \tag{1}$$

where the subscripts "fc," "eq," and "hot" refer to the nuclear degrees of freedom and denote Franck-Condon, equilibrated, and nonequilibrated states, respectively. The dynamical processes in Eq. (1) are predicted to be reflected in the spectroscopy via (i) the "bleach" and recovery in the $s \rightarrow p$ absorption and (ii) the dynamical evolution of the p-state absorption, which *blueshifts* from the mid-IR at early times to the near-IR and visible during the p-state fc $\rightarrow$ eq adiabatic solvation.

According to this model, both the absorption transitions are significant at all the probe wavelengths reported in Fig. 1. For example, at 920 nm the data exhibit an initial $s \rightarrow p$ bleach followed by a delayed absorption of the p state, as it blueshifts into the probe wavelength region. The ~1 ps decay time of the 920 nm absorption is assigned to the $p \rightarrow s$ nonadiabatic transition [3]. The situation is very different at 780 nm; here the initial $s \rightarrow p$ bleach is almost exactly canceled by the p_{eq} absorption and the dynamics primarily reflect the p-state adiabatic solvation, not the nonadiabatic transition. At the shorter probe wavelengths, 720 nm, the $s \rightarrow p$ bleach

 0031-9007/98/80(5)/1086(4)$15.00

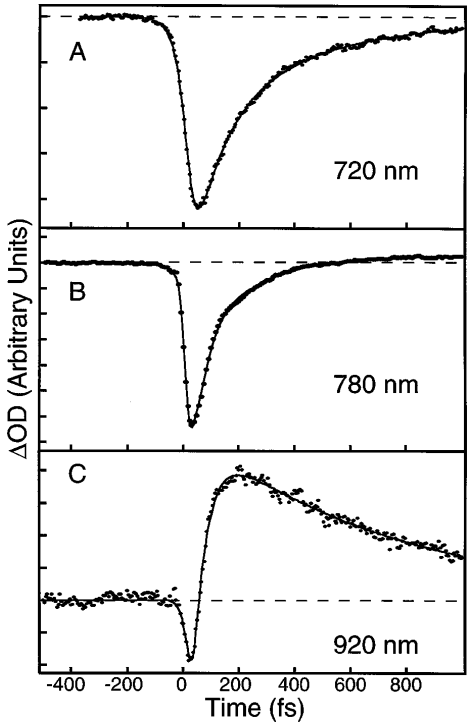

FIG. 1. Transient ΔOD (change in optical density) signal of the hydrated electron in 10 mM $K_4Fe(CN)_6$ aqueous solution, which was flowed in a ~0.3 mm jet. The 800 nm, 1–2 μJ linearly polarized pump pulse was oriented at 54.7° with respect to the polarization of the probe pulse. The probe wavelengths, selected from a single filament white-light continuum generated in sapphire, are indicated in each panel. A small (1%–5%) artifact due to pump-probe cross-phase modulation was observed in the data. The cross-phase modulation signal was determined separately by measuring the pump-probe signal in the absence of solvated electrons (no 263.5 nm photoejection pulse), and the data were corrected for this small artifact. The solid lines through the data are convolutions of the instrument response function with a model for the dynamics; see Table I.

is only partially canceled by the p-state absorption, and the dynamics reflect both p-state adiabatic solvation and $s \rightarrow p$ nonadiabatic transition. In addition, the spectral evolution of the p-state absorption, as manifested in the average solvation time $\langle\tau\rangle$, is most rapid at the longest wavelength probed, and becomes slower at shorter probe wavelengths; see Table I. This is qualitatively consistent with theoretical expectations that the p-state absorption undergoes a dramatic blueshift during solvation. Further evidence that the <300 fs dynamics is associated with adiabatic solvation dynamics is the H_2O/D_2O solvent isotope effect on the kinetics.

It is informative to compare the experimental results to predictions of recent quantum molecular dynamics simulations. The simulations predict transient features due to adiabatic solvation involving initial inertial solvent motion followed by a slower diffusional solvent motion. Published simulations of the pump-probe spectroscopy have been convoluted with a 300 fs instrument response function to compare with previous experiments, so a detailed comparison of the results with theory will require new simulations. The time-dependent quantum s-p energy gap from the simulations has been analyzed to determine the nonequilibrium solvent response function $S(t)$, which measures equilibration of the p state [4]. The simulated $S(t)$ was well fit by a model function comprised of a Gaussian decay (~25 fs, ~38% amplitude; inertial motion of the H_2O molecules), followed by an exponential decay (~250 fs diffusive solvation). These time scales are also in agreement with adiabatic molecular dynamics (MD) simulations of excess electrons in water clusters by Barnett *et al.* in which an equilibrated, ground-state excess electron was suddenly switched to a p-like state [16]. MD simulations by Staib and Borgis on the hydrated electron in flexible, polarizable water, involving equilibrium solvation dynamics, predict a 12 fs Gaussian component and a 130 fs exponential component [7]. Related polar solvation molecular dynamics simulations on photoexcited fluorescent probes are predicted to exhibit solvation dynamics associated with both inertial solvent motion (25 fs) and diffusional solvation on the hundreds of femtosecond time scales [25], and experiments exhibit solvation on the ≤55 fs (48%), 126 fs (20%), and 880 fs (35%) time scales [26].

TABLE I. Fit parameters of the model function, $\Delta\text{OD} = A_G \exp(-t^2/2\tau_G^2) + A_1 \exp(-t/\tau_1) + A_2 \exp(-t/\tau_2)$, to the pump-probe signals (change in optical density) for excess electrons in H_2O and in D_2O at 288 ± 2 K.[a]

Solvent	λ (nm)	τ_G (fs)	A_G	τ_1 (fs)	A_1	τ_2 (fs)	A_2	$\langle\tau\rangle$ (fs)[b]
H_2O	720	79 ± 5	−0.26 ± 0.03	263 ± 9	−0.65 ± 0.05	630 ± 43	−0.09 ± 0.02	215 ± 5
	780	51 ± 6	−0.47 ± 0.04	220 ± 12	−0.47 ± 0.03	2140 ± 433	0.06 ± 0.01	142 ± 11
	800	69 ± 9	−0.30 ± 0.08	194 ± 24	−0.60 ± 0.08	2049 ± 332	0.10 ± 0.01	156 ± 12
	820	58 ± 7	−0.32 ± 0.06	173 ± 16	−0.56 ± 0.06	1807 ± 76	0.11 ± 0.01	154 ± 13
	920	32 ± 8	−0.28 ± 0.1	99 ± 21	−0.39 ± 0.10	814 ± 116	0.33 ± 0.02	73 ± 11
D_2O	720	120 ± 13	−0.19 ± 0.06	271 ± 27	−0.73 ± 0.08	905 ± 200	−0.08 ± 0.07	244 ± 16
	780	75 ± 10	−0.38 ± 0.05	222 ± 23	−0.54 ± 0.06	2007 ± 678	0.08 ± 0.01	169 ± 13
	800	102 ± 6	−0.29 ± 0.08	210 ± 27	−0.59 ± 0.08	1705 ± 319	0.12 ± 0.01	181 ± 12
	820	97 ± 9	−0.33 ± 0.08	185 ± 23	−0.52 ± 0.09	1631 ± 234	0.15 ± 0.02	159 ± 10

[a]The sum of individual amplitudes was normalized to unity. The errors are 1 standard deviation from the mean of multiple measurements (typically >20).

[b]The average time constant is defined by $\langle\tau\rangle = (\sqrt{\frac{\pi}{2}} A_G \tau_G + A_1 \tau_1)/(A_G + A_1)$.

It is encouraging that τ_G and τ_1 values (Table I) are close to the expected time scales of the simulated solvent response function $S(t)$, e.g., especially at a probe wavelength of 920 nm. Indeed, trial functions consisting of a sum of a Gaussian and an exponential for solvation (consistent with theory), and an additional exponential for the p-state population decay, give an excellent fit to the data [see Fig. 2(B)]. The fit is significantly better than a function consisting of the sum of three exponentials. The discrepancy between the observed τ_G of 50–68 fs in H_2O in the visible region and the predicted ~25 fs time scale for $S(t)$ may be due to several factors, including a failure of the absorption at a particular wavelength to be linearly proportional to the evolving p-s energy gap, a failure of the theoretical models for the solvation dynamics time scales, non-Condon effects in the absorption intensity, or the possible involvement of relaxation among the p levels in the actual experiment. The new spectrometer has sufficient time resolution to rule out a spectral component in the 25 fs time scale as demonstrated in Fig. 2(D), where a simulated transient with the Gaussian component constrained to 25 fs (dashed line) is shown to evolve more rapidly than the experimental data points.

Isotope effects on the various time scales and processes for the solvated electron offer an important means of testing theoretical predictions. The Gaussian component (τ_G, Table I) is observed to be especially sensitive to solvent deuteration (45%–65% longer in D_2O than in H_2O for the wavelengths where the isotope effect was investigated). The amplitude-weighted average time constant $\langle\tau\rangle = (\sqrt{\frac{\pi}{2}}\,A_G\tau_G + A_1\tau_1)/(A_G + A_1)$ shows a smaller isotope effect, ranging from 19% at 780 nm to 3% at 820 nm. Conflicting predictions on the magnitude of isotope effects emerge from the MD simulations. In simulations by Barnett *et al.*, the inertial component of the evolution of the quantum energy gap was longer by $2^{1/2}$ in D_2O due to solvent librations (hindered rotations) [16]. In the nonadiabatic MD simulations of Schwartz and Rossky the Gaussian component shows a much smaller isotope effect (≤10%) [5]. This was rationalized with the interpretation that mostly translational solvent modes are involved in accommodating the p-like shape and charge distribution after photoexcitation—see also Graf *et al.* for related studies [18]. The isotope effects on the Gaussian components reported in this Letter suggest that librational motions are responsible for the inertial dynamics. The absence of an observed isotope effect for the $p \rightarrow s$ decay rate is consistent with recent theoretical work, including that of Rossky, that has demonstrated the importance of quantum decoherence in the radiationless decay process [6,27]. Another interesting aspect of the experimental data is apparent in the manifestation of coherent wave packet dynamics that are marked by an asterisk in Fig. 2(E). This type of feature was recently identified and assigned to wave packet dynamics by Wiersma *et al.* (preliminary results) [28]. The features in Fig. 2(E) are highly reproducible and not the consequence of pump-induced cross-phase modulation of the probe, which is negligible at 820 nm in these experiments. The results are qualitatively consistent with a rapidly dephased librational wave packet in the s state, launched by the leading edge of the pump pulse by resonant impulsive stimulated Raman scattering [29]. This exciting preliminary result, which opens the door to the first vibrational spectroscopy of the hydrated electron, will undoubtedly be the subject of future investigation.

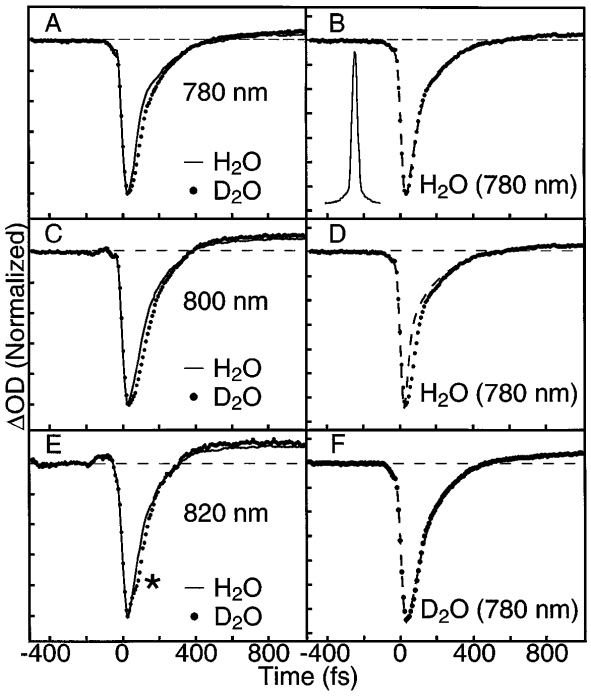

FIG. 2. Similar to Fig. 1, except the probe-pulse light was derived directly from the amplified laser and wavelength filtered after the sample with ±5 nm interference filters.

In summary we have performed the first femtosecond measurements on the hydrated electron with sufficient time resolution to observe inertial solvation dynamics. The comparison with nonadiabatic quantum molecular dynamics simulations supports the general validity of the theoretical treatments and leads to new insights on the molecular details of the solvation relaxation processes of the hydrated electron.

We thank Donghee Son for his assistance in collecting some of the data reported herein. We acknowledge Sterling Backus for his advice on the construction of the Ti:sapphire multipass laser system. This research was funded by a grant from the BES-OER Program of the DOE and the NSF.

*Corresponding author.
Electronic address: barbara@chem.umn.edu

[1] E. Neria, A. Nitzan, R. N. Barnett, and U. Landman, Phys. Rev. Lett. **67**, 1011 (1991).

[2] B. J. Schwartz and P. J. Rossky, Phys. Rev. Lett. **72**, 3282 (1994).
[3] B. J. Schwartz and P. J. Rossky, J. Chem. Phys. **101**, 6917 (1994).
[4] B. J. Schwartz and P. J. Rossky, J. Chem. Phys. **101**, 6902 (1994).
[5] B. J. Schwartz and P. J. Rossky, J. Chem. Phys. **105**, 6997 (1996).
[6] B. J. Schwartz, E. R. Bittner, O. V. Prezhdo, and P. J. Rossky, J. Chem. Phys. **104**, 5942 (1996).
[7] A. Staib and D. Borgis, J. Chem. Phys. **103**, 2642 (1995).
[8] S. Bratos and J.-C. Leicknam, Chem. Phys. Lett. **261**, 117 (1996).
[9] S. Bratos, J.-C. Leicknam, D. Borgis, and A. Staib, Phys. Rev. E **55**, 7217 (1997).
[10] L. Turi, P. Holpar, E. Keszei, C. Pépin, and D. Houde, J. Phys. Chem. A **101**, 5469 (1997).
[11] C. Pépin, T. Goulet, D. Houde, and J. P. Jay-Gerin, J. Phys. Chem. A **101**, 4351 (1997).
[12] R. A. Crowell and D. M. Bartels, J. Phys. Chem. **100**, 17 940 (1996).
[13] X. Shi, F. H. Long, H. Lu, and K. B. Eisenthal, J. Phys. Chem. **100**, 11 903 (1996).
[14] A. Reuther, A. Laubereau, and D. N. Nikogosyan, J. Phys. Chem. **100**, 16 794 (1996).
[15] H. Gelabert and Y. Gauduel, J. Phys. Chem. **100**, 13 993 (1996).
[16] R. B. Barnett, U. Landman, and A. Nitzan, J. Chem. Phys. **90**, 4413 (1989).
[17] E. Neria and A. Nitzan, J. Chem. Phys. **99**, 1109 (1993).
[18] P. Graf, A. Nitzan, and G. H. F. Diercksen, J. Phys. Chem. **100**, 18 916 (1996).
[19] I. Rips, Chem. Phys. Lett. **245**, 79 (1995).
[20] J. Schnitker, K. Motakabbir, P. J. Rossky, and R. Friesner, Phys. Rev. Lett. **60**, 456 (1988).
[21] A. Wallqvist, G. Martyna, and B. J. Berne, J. Phys. Chem. **92**, 1721 (1988).
[22] J. C. Alfano, P. K. Walhout, Y. Kimura, and P. F. Barbara, J. Chem. Phys. **98**, 5996 (1993).
[23] Y. Kimura, J. C. Alfano, P. K. Walhout, and P. F. Barbara, J. Phys. Chem. **98**, 3450 (1994).
[24] S. Backus, J. Peatross, C. P. Huang, M. M. Murnane, and H. C. Kapteyn, Opt. Lett. **20**, 2000 (1995).
[25] M. Maroncelli and G. R. Fleming, J. Chem. Phys. **89**, 5044 (1988).
[26] G. R. Fleming and M. Cho, Annu. Rev. Phys. Chem. **47**, 109 (1996).
[27] E. R. Bittner, B. J. Schwartz, and P. J. Rossky, Theochem. J. Mol. Struct. **389**, 203 (1997).
[28] D. A. Wiersma (private communication).
[29] K. A. Nelson, in *Raman Spectroscopy: Sixty Years on Vibrational Spectra and Structure*, edited by H. D. Bist, J. R. Durig, and J. F. Sullivan (Elsevier Science, Amsterdam, 1989), Vol. 17B, p. 83.